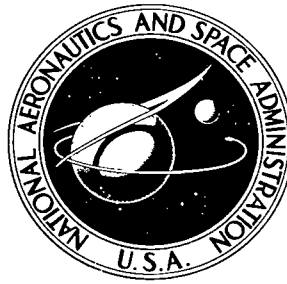


NASA TECHNICAL NOTE



NASA TN D-4413

e.1

NASA TN D-4413



LOAN COPY; RETURN  
AT THE (YAL11-2)  
BELL AND HOWELL

# FEASIBILITY OF SUPPORTING LIQUID FUEL ON A SOLID WALL IN A RADIATING LIQUID-CORE NUCLEAR ROCKET CONCEPT

*by Henry A. Putre and Albert F. Kascak*

*Lewis Research Center*

*Cleveland, Ohio*

TECH LIBRARY KAFB, NM



0131351

FEASIBILITY OF SUPPORTING LIQUID FUEL ON A SOLID WALL  
IN A RADIATING LIQUID-CORE NUCLEAR ROCKET CONCEPT

By Henry A. Putre and Albert F. Kascak

Lewis Research Center  
Cleveland, Ohio

NATIONAL AERONAUTICS AND SPACE ADMINISTRATION

---

For sale by the Clearinghouse for Federal Scientific and Technical Information  
Springfield, Virginia 22151 - CFSTI price \$3.00

# FEASIBILITY OF SUPPORTING LIQUID FUEL ON A SOLID WALL IN A RADIATING LIQUID-CORE NUCLEAR ROCKET CONCEPT

by Henry A. Putre and Albert F. Kascak

Lewis Research Center

## SUMMARY

A reference liquid fuel nuclear rocket concept, previously analyzed, consists of a liquid carbide fuel mixture supported on the inside wall of a rotating tube. Most of the nuclear heat generated in the liquid fuel is radiated to the axially flowing hydrogen propellant. A fraction of this heat generation, called the wall cooling ratio, is removed by support-wall cooling. The reference engine delivered a 1430-second specific impulse, with a  $9500^{\circ}\text{R}$  ( $5280^{\circ}\text{K}$ ) radiating surface temperature, and a 25-percent wall cooling ratio. Solid-support-wall temperature for this rocket, assuming only simple molecular conduction in the liquid fuel, was estimated as  $14\,500^{\circ}\text{R}$  ( $8000^{\circ}\text{K}$ ), which of course, greatly exceeds structural material limits.

This report extends the original liquid fuel heat-transfer analysis for the reference engine by developing an expression for combined molecular and propellant induced turbulent heat transfer in the liquid fuel, and results in a more rigorous determination of support-wall temperature. In addition, two means of reducing support-wall temperature without severely affecting rocket performance are investigated.

For the reference fuel-element configuration, with uniform heat source distribution in the liquid fuel, the support-wall temperature calculated from the more complete turbulent analysis was  $9830^{\circ}\text{R}$  ( $5460^{\circ}\text{K}$ ), which is well above currently practical wall material limits.

When the fuel was zoned into a region in the liquid near the propellant interface, the support-wall temperature was found to be about  $1200^{\circ}\text{R}$  ( $670^{\circ}\text{K}$ ) lower than for the unzoned case. A simplified mass-transfer analysis indicates, however, that fuel zoning cannot be maintained over rocket lifetime, and therefore wall temperature reduction by fuel zoning does not appear feasible.

The insulating effect of a stable opaque vapor layer built up at the solid-liquid interface was also evaluated. Wall temperature was found to be reduced to  $8500^{\circ}\text{R}$  ( $4720^{\circ}\text{K}$ ) at 1430 seconds specific impulse by the vapor layer. Current wall materials, such as graphite used at  $7200^{\circ}\text{R}$  ( $4000^{\circ}\text{K}$ ) in conjunction with an opaque vapor layer, may permit operation at a reduced specific impulse of about 1250 seconds.

## INTRODUCTION

For planetary space missions and short trip times, a high specific impulse and moderate thrust rocket is necessary. Reference 1 describes such a nuclear rocket, which employs a bundle of rotating liquid fuel elements with the liquid niobium carbide (NbC) and uranium carbide (UC<sub>2</sub>) mixture supported on solid cylindrical walls by centripetal acceleration. Figure 1(a) shows one of the fuel elements. The propellant flows axially through the center of the annular liquid fuel element, and it is heated by thermal radiation from the liquid surface.

The ultimate goal of this rocket is to heat the propellant to as high a temperature as possible with minimum mass transfer from the liquid fuel element to the propellant. The fuel temperature is chosen sufficiently high so that thermal radiation is the dominant mode of heat transfer, thus almost uncoupling heat and mass transfer.

Reference 1 showed that from cycle considerations, the percent of heat removed through the solid wall by regenerative cooling strongly affected the rocket specific impulse. In fact, for maximum specific impulse this wall cooling ratio must be kept to a minimum (see table I). With reduced wall cooling, however, the temperature of the

TABLE I. - WALL COOLING RATIO  
AND SPECIFIC IMPULSE FOR  
3500° R PROPELLANT  
TEMPERATURE AT  
FUEL-ELEMENT  
INLET (FROM  
REF. 1)

Wall cooling ratio, $\eta$	Specific impulse, $I_{sp}$ , sec
0.2	1570
.25	1430
.3	1280
.4	1110
.5	1000

inner solid wall surface tends to increase above the wall material structural limit. The feasibility of this rocket concept then rests on the possibility of finding a compromise between these two limits.

The reference engine evolved in reference 1 had a 1430-second specific impulse with a radiating surface temperature of 9500° R (5280° K). Twenty-five percent of the nuclear heat generation had to be removed by cooling the solid wall and surrounding structure.

An estimate of solid support-wall temperatures for this engine, considering only molecular conduction in the liquid fuel, indicated that the wall temperature ( $14\ 400^{\circ}\text{R}$ ,  $8000^{\circ}\text{K}$ ) greatly exceeded structural material limits and that the fuel would boil internally.

The analysis in reference 1 had several shortcomings, but it did serve to show that turbulent effects in the liquid fuel mixture should be considered in a determination of support-wall temperatures. The objectives of this report are to extend the liquid fuel heat-transfer analysis of reference 1 by including turbulence, and to determine accurately support-wall temperature at design performance conditions. Specific questions to be answered in this report are the following:

- (1) With turbulent convection in the liquid fuel properly accounted for, do support-wall temperatures fall within realistic material limits?
- (2) Are support-wall temperatures significantly reduced by zoning the fuel into a region in the liquid away from the support wall?
- (3) Could an opaque vapor layer built up at the liquid-solid interface reduce support-wall temperature to within realistic limits? The maximum stable vapor-layer thickness is estimated from a simple vapor bubble force balance.

With these objectives in mind, the liquid-fuel-element configuration of reference 1, illustrated in figure 1(b), was analyzed. Design values from reference 1 which will be used in this study are given in table II.

TABLE II. - DESIGN VALUES FOR LIQUID-CORE  
NUCLEAR ROCKET FROM REFERENCE 1

Fuel mixture temperature at gas surface, $T_1$	$9500^{\circ}\text{R}$ ( $5280^{\circ}\text{K}$ )
Radiant heat flux from liquid-fuel mixture to gas stream, $q_1'$	$3.52 \times 10^7\ \text{J}/(\text{m}^2)(\text{sec})$
Rocket specific impulse, $I_{sp}$	1430 sec
Wall cooling ratio, $\eta$	0.25
Thickness of liquid-fuel mixture, $L$	0.0095 m
Inner radius of fuel-element solid support wall, $R$	0.060 m
Rotational speed of fuel-element support wall, $\omega$	2400 rpm
Radial acceleration due to element rotation, $g_r$	378 $g_0$
Propellant mass velocity, $G_g$	$33.0\ \text{kg}/(\text{m}^2)(\text{sec})$
Propellant density, $\rho_g$	$1.47\ \text{kg}/\text{m}^3$

## SYMBOLS

- A ratio of eddy to molecular thermal conductivity at  $y = L$   
 $a_R$  Rosseland mean radiative absorption coefficient

$C$	mole fraction of uranium carbide in liquid fuel mixture
$C_o$	value of $C$ at solid wall
$\bar{C}$	value of $C$ averaged over the liquid fuel thickness
$c_{P_L}$	liquid specific heat
$D$	molecular mass diffusion coefficient
$d$	diameter of vapor bubble at solid wall, see fig. 3(a)
$d_b$	vapor bubble base diameter, see fig. 3(a)
$f_g$	pipe friction factor for gas stream
$G_g$	gas mass velocity
$g_o$	gravitational acceleration constant, $9.80 \text{ m/sec}^2$
$g_r$	radial acceleration
$I_{sp}$	specific impulse, defined as thrust per unit weight flow rate at $g_o$ , sec
$K(r)$	generalized total thermal conductivity
$k_L$	molecular thermal conductivity
$L$	thickness of liquid fuel mixture
$Pr_L$	liquid Prandtl number
$Q$	constant for nuclear heat generation rate per unit volume
$q_o''$	heat flux from liquid fuel mixture to solid wall
$q'''(r)$	generalized nuclear heat generation rate per unit volume
$q_1''$	heat flux from liquid fuel mixture to gas stream
$R$	inner radius of fuel-element solid wall
$r$	distance from fuel-element centerline
$S$	equivalent surface roughness
$T$	liquid-fuel-mixture temperature
$T_o$	fuel-mixture surface temperature facing the solid wall
$T_1$	fuel-mixture temperature at gas surface
$T_w$	solid-wall temperature at inner surface
$t$	time
$t_{1/2}$	real time corresponding to $\theta_{1/2}$

$u_L^*$	$\sqrt{\tau/\rho_L}$ liquid-fuel-mixture friction velocity
$y$	distance in liquid fuel mixture measured from solid wall
$y^+$	$y^+ = (yu_L^*/\nu_L)$ , dimensionless value corresponding to $y$
$\alpha$	dimensionless pipe roughness parameter, $\alpha = S/L$
$\beta$	fraction of liquid thickness which has no heat sources
$\delta$	vapor-layer thickness
$\epsilon_H$	liquid eddy thermal diffusivity
$\epsilon_m$	liquid eddy momentum diffusivity
$\eta$	ratio of heat removed at solid wall to total heat generated
$\theta$	dimensionless time, $\theta = Dt/L^2$
$\theta_{1/2}$	dimensionless time when $C_o/\bar{C} = 0.5$
$\mu_L$	liquid viscosity
$\nu_L$	liquid kinematic viscosity, $\nu_L = \mu_L/\rho_L$
$\rho_g$	gas density
$\rho_L$	liquid density
$\sigma$	liquid-fuel-mixture surface tension
$\tau$	gas shear stress at liquid-gas interface
$\varphi$	contact angle at base of vapor bubble, see fig. 3(a)
$\chi$	optical thickness, number of radiation mean free paths
$\omega$	fuel-element angular velocity

## ANALYSIS

Since this report treats several separate but related problems, as indicated in the INTRODUCTION, the analysis of these problems is presented in several separate sections. The relevancy of each of the various analysis sections is discussed in greater detail as part of the RESULTS AND DISCUSSION.

The first analysis derives the temperature distribution in the liquid fuel mixture, with turbulent heat transport included, for a generalized step distribution of heat sources due to nuclear fuel zoning. The next section (p. 17) derives the fuel concentration distribution in the liquid mixture as a function of time from rocket startup for various cases

of initial fuel zoning. The final section (p. 18) uses a radiative heat-transfer analysis to calculate the temperature drop across a stable, insulating, opaque vapor layer built up at the liquid-solid interface.

## LIQUID-FUEL-MIXTURE TEMPERATURE PROFILES WITH ZONED HEAT SOURCES AND TURBULENT HEAT TRANSPORT

The temperature profiles in the liquid fuel mixture and the wall temperature  $T_w$  are calculated for the fuel element model illustrated in figure 1(b) using the reference design radiating surface temperature and heat flux and the range of wall cooling ratios in reference 1. This calculation requires that heat source and thermal conductivity distributions are specified throughout the liquid. The heat diffusion equation with only radial steady-state heat transfer is considered. In the most general case, both the heat source strength and thermal conductivity vary radially. The generalized thermal conductivity includes both molecular and eddy heat transport.

The generalized heat-transfer relation for the liquid fuel mixture then is

$$\frac{1}{r} \frac{d}{dr} \left[ rK(r) \frac{dT}{dr} \right] + q'''(r) = 0 \quad (1)$$

The boundary conditions from figure 1(b) at  $r = (R - L)$  are

$$T = T_1 = 9500^\circ \text{ R } (5280^\circ \text{ K}) \quad (2)$$

$$K(r) \frac{dT}{dr} = q_1'' = 3.52 \times 10^7 \frac{\text{J}}{(\text{m}^2)(\text{sec})} \quad (3)$$

(These design values are given in table II.)

Temperature profile solutions are seen to be physically realistic to the extent that expressions for  $q'''(r)$  and  $K(r)$  apply. Thus these quantities must be carefully considered. The heat source term  $q'''(r)$  is by definition related to the wall cooling ratio  $\eta$  and the gas interface heat flux  $q_1''$  by the equation

$$\int_{R-L}^R r q'''(r) dr = q_1'' (R - L) + q_0'' R = q_1'' \left( \frac{R - L}{1 - \eta} \right) \quad (4)$$

For the case of zoned nuclear fuel, a step heat source distribution is assumed with a

uniform nonzero heat source in the region  $\beta L < y < L$ , as indicated in figure 1(b). With this zoned heat source distribution and equation (4), expression for equation (1), rewritten in terms of  $\eta$  and  $q_1'$  with  $y$  measured from the support wall, becomes, for  $0 < y < \beta L$ ,

$$q'''(r) = 0 \quad (5)$$

and for  $\beta L < y < L$ ,

$$q'''(r) = Q = \frac{2q_1'(R - L)}{(1 - \eta) \left[ (R - \beta L)^2 - (R - L)^2 \right]} \quad (6)$$

An important phenomenon now considered is that of turbulent mixing in the liquid fuel mixture. The objective is to derive expressions for shear stress and finally eddy diffusivity in the liquid fuel mixture. From studies of liquid-gas surface interaction in annular two-phase flow, it is well known that, with a turbulent gas stream flowing over a thin liquid film, the turbulent gas eddies interact with the liquid surface. They thereby transfer their random mixing motion to the liquid. By postulating that the liquid-film surface in annular two-phase flow affects the gas like a rough-wall pipe, Wrobel and McManus (ref. 2) were able to show that a shear stress could be calculated at the liquid-gas interface from known values of gas Reynolds number and liquid-film thickness. Reference 2 also showed that this shear stress could be used to find the velocity distribution and eddy viscosity in the liquid film.

Similar liquid-gas surface interactions are assumed to occur in the liquid-fuel-element configuration; then, turbulent mixing in the liquid fuel mixture is an important mechanism for heat transfer. An expression for liquid fuel eddy thermal conductivity is derived with the aid of the analysis of reference 2.

The liquid fuel acts on the propellant gas like a rough-wall pipe having an equivalent roughness equal to some fraction  $\alpha$  of the liquid thickness, or

$$S = \alpha L \quad (7)$$

With this surface roughness used in a rough-wall-pipe friction factor correlation and with the hydrogen propellant velocity given in table II, the interfacial shear stress can be calculated. The friction factor correlation for rough-wall pipes is given in reference 3 (p. 525); for the gas stream it takes the form

$$f_g = \frac{1}{\left[ 2 \log \left( \frac{R - L}{S} \right) + 1.74 \right]^2} \quad (8)$$

The correct value of  $\alpha$  to be used in equation (7) depends on the wave structure of the liquid surface. Based on the work of reference 2, a value of  $\alpha = 1/2$  gives at worst an underestimate of gas friction factor and liquid turbulence level, and therefore, it is used here. A more accurate value of  $\alpha$  requires detailed experimental study of the gas-liquid surface interaction. Such a study was not considered here since the end results are quite insensitive to the exact value of  $\alpha$ .

The gas friction factor calculated from equations (7) and (8), using design values from table II, becomes

$$f_g = 0.070 \quad (9)$$

The gas shear at the gas-liquid interface in terms of gas mass velocity and friction factor is

$$\tau = \frac{f_g G_g^2}{8\rho_g} \quad (10)$$

The liquid fuel eddy viscosity can now be calculated assuming this interfacial shear value applies for the entire liquid thickness, and that this shear stress leads to turbulent mixing in the liquid fuel similar to mixing in developed pipe flow for the same shear stress. The eddy viscosity can be derived from the universal velocity distribution given in reference 3 (p. 509) with the following results:

For  $y^+ \leq 5$  (laminar sublayer),

$$\epsilon_m = 0 \quad (11)$$

For  $y^+ \geq 70$  (turbulent region),

$$\epsilon_m = \nu_L (0.4y^+ - 1) \quad (12)$$

where

$$y^+ = \frac{yu_L^*}{\nu_L} \quad (13)$$

and

$$u_L^* = \sqrt{\frac{\tau}{\rho_L}} = \sqrt{\frac{f_g(G_g)^2}{8\rho_L\rho_g}} \quad (14)$$

For simplicity and for purposes here, equation (12) is assumed to apply over the region  $5 < y^+ < 70$ . Invoking the Reynolds analogy between turbulent momentum and heat transfer, or  $\epsilon_H = \epsilon_m$ , gives the expression for thermal conductivity including turbulent mixing as

$$K(r) = k_L \quad y^+ \leq 5 \quad (15)$$

$$K(r) = k_L \left[ 1 + \text{Pr}_L (0.4 y^+ - 1) \right] \quad y^+ > 5 \quad (16)$$

Using liquid-fuel-mixture properties from the appendix and design values from table II enables equations (15) and (16) to be rewritten in the nearly equivalent form

$$K(r) = k_L \left( 1 + A \left( \frac{y}{L} \right) \right) \quad (17)$$

where the calculated value of the turbulence coefficient is

$$A = 11.0 \quad (18)$$

This variation of total thermal conductivity across the liquid thickness is shown in figure 2. As is generally found in turbulent boundary layer flows, total thermal conductivity increases linearly from the solid wall (see fig. 2).

Using the total thermal conductivity in the form of equation (17) together with the heat source terms of equations (5) and (6) in the basic heat-transfer equations (1), (2), and (3), and satisfying temperature and heat flux continuity at  $y = \beta L$  yield the temperature solution for the zoned fuel case with turbulent conduction:

For  $0 \leq y \leq \beta L$ :

$$T = T(y = \beta L) - \frac{Q\eta L}{2k_L} \left[ \frac{(R - \beta L)^2 - (R - L)^2}{L + AR} \right] \left[ \ln \frac{R - y}{R - \beta L} - \ln \frac{1 + A \frac{y}{L}}{1 + A\beta} \right] \quad (19)$$

For  $\beta L < y \leq L$ :

$$T = T_1 + \frac{QL}{2k_L} \left\{ \left[ \frac{(1 - \eta)(R - \beta L)^2 + \eta(R - L)^2}{L + AR} \right] \left[ \ln \frac{R - y}{R - L} - \ln \frac{1 + A \frac{y}{L}}{1 + A} \right] + \frac{L}{A^2} \left[ A \left( 1 - \frac{y}{L} \right) + \left( 1 + \frac{AR}{L} \right) \ln \frac{1 + A \frac{y}{L}}{1 + A} \right] \right\} \quad (20)$$

where

$$T(y = \beta L) = T_1 + \frac{QL}{2k_L} \left\{ \left[ \frac{(1 - \eta)(R - \beta L)^2 + \eta(R - L)^2}{L + AR} \right] \left[ \ln \frac{R - \beta L}{R - L} - \ln \frac{1 + A\beta}{1 + A} \right] + \frac{L}{A^2} \left[ A(1 - \beta) + \left( 1 + \frac{AR}{L} \right) \ln \frac{1 + A\beta}{1 + A} \right] \right\} \quad (21)$$

## TIME DEPENDENCE OF ZONED FUEL CONCENTRATIONS

The time dependence of zoned fuel concentrations is calculated by assuming a simple one-dimensional diffusion model. Referring to figure 1(b), and assuming a constant value of diffusion coefficient and a small molar fuel concentration compared to solvent concentration, yields the mass diffusion equation with initial and boundary conditions for the fuel species as

$$\frac{\partial^2 C}{\partial y^2} = \frac{1}{D} \frac{\partial C}{\partial t} \quad (22)$$

Initial conditions:

At  $t = 0$ ,

$$C = 0 \quad 0 < y < \beta L \quad (23)$$

$$C = \left( \frac{\bar{C}}{1 - \beta} \right) \quad \beta L < y < L \quad (24)$$

Boundary conditions:

At  $y = 0$ ,

$$\frac{\partial C}{\partial y} = 0 \quad (25)$$

and at  $y = L$ ,

$$\frac{\partial C}{\partial y} = 0 \quad (26)$$

The quantity  $\bar{C}$  in equation (24) is the equilibrium fuel concentration averaged over the liquid mixture thickness. The actual value of  $\bar{C}$  is not important here; however, for purposes herein, it remains constant for all values of  $\beta$ . When the separation of variables method is used, the solution to equations (22) to (26) is

$$\frac{C}{\bar{C}} = 1 - \frac{2}{\pi(1 - \beta)} \sum_{n=1}^{\infty} \left[ \frac{\sin(n\pi\beta) \cos\left(n\pi \frac{y}{L}\right) e^{-\eta^2 \pi^2 \theta}}{n} \right] \quad (27)$$

where  $\theta$  is the dimensionless time variable

$$\theta = \frac{Dt}{L^2} \quad (28)$$

Equation (27) evaluated at the wall becomes

$$\frac{C_o}{\bar{C}} = 1 - \frac{2}{\pi(1 - \beta)} \sum_{n=1}^{\infty} \left[ \frac{\sin(n\pi\beta)e^{-n^2\pi^2\theta}}{n} \right] \quad (29)$$

## VAPOR INSULATOR BETWEEN LIQUID AND SOLID REGIONS

One method of reducing support-wall temperature is by means of an insulating vapor layer built up between the support wall and the liquid fuel. Conceptually the vapor layer would form either by sublimation of the solid wall or by gas injection through the solid wall. The stable thickness of such a vapor layer is difficult to estimate in view of the complicated two-phase flow structure; however, an approximate value of the maximum stable vapor layer thickness is derived from a single vapor bubble force balance.

The principal forces acting on a vapor bubble attached to the solid wall in the centrepetal gravitational field are assumed to be the bouyancy and surface tension forces. Then, with a spherical bubble shape assumed as shown in figure 3, the force balance at detachment is

$$\rho_L \frac{\pi d^3}{6} g_r = \pi \sigma d_b \sin \varphi \quad (30)$$

The quantity  $d_b \sin \varphi$  is approximated by the bubble diameter. The maximum stable vapor thickness is assumed to be equal to the bubble diameter at detachment.

The maximum stable vapor thickness is thus given by

$$\delta = d = \sqrt{\frac{6\sigma}{\rho_L(g_r)}} \quad (31)$$

Using the value of  $g_r = 387 g_o$  from reference 1 and the fuel mixture properties given in the appendix yield

$$\delta = 0.57 \text{ mm} \quad (32)$$

This estimate of the maximum vapor thickness is probably an overestimate since fluid dynamical forces on the bubble, which tend to sweep the bubble off the solid wall, have been neglected.

The temperature drop across this vapor layer can be calculated. Since radiation is the dominant mode of heat transfer from the liquid fuel to the propellant, only radiative heat transfer is assumed through the vapor layer. (This is equivalent to assuming that the thermal conductivity of the vapor times the temperature gradient is small compared to the amount of heat transferred by radiation.) The diffusion analysis of reference 4 for radiative heat transfer across an absorbing medium between flat plates is used, with the walls assumed black. This analysis requires that the optical thickness be specified.

The optical thickness  $\chi$  of the stable vapor layer just described is now estimated from the definition

$$\chi \equiv \int_0^{\delta} a_R dy \quad (33)$$

The determination of  $\chi$  requires that the vapor composition and the absorption coefficient of its various species be known. The composition of the vapor is very difficult to determine since the diffusion process is nonisothermal. If this vapor has a constant absorption coefficient, then  $\chi$  is given by the product of the absorption coefficient and the vapor thickness:

$$\chi = a_R \delta$$

Using the value of  $a_R$  ( $3.2 \text{ mm}^{-1}$ ) for carbon vapor at 200 atmospheres ( $2.02 \times 10^7 \text{ N/m}^2$ ) and  $9000^\circ \text{ R}$  ( $5000^\circ \text{ K}$ ) based on reference 5 gives  $\chi = 1.8$ .

It is difficult to assess the accuracy of this estimate of the vapor opacity. Photoionization and atomic line absorption are normally considered unimportant at temperatures less than  $10\,000^\circ \text{ K}$ ; molecular transition absorption should be dominant. The absorption coefficient is thus characterized by a great number of lines. This creates the possibility of a window in the absorption spectrum. The possibility of this window plus the strong temperature dependent properties would seem to overshadow the neglect of some of the molecular species present; thus, the present estimated  $\chi$  is probably too high.

## RESULTS AND DISCUSSION

The preceding analysis was applied to the liquid-core nuclear rocket described in reference 1, which consists of a liquid carbide fuel mixture supported on the inside wall

of a rotating tube. The axially flowing hydrogen propellant is heated by thermal radiation from the liquid surface. For purposes here, engine design values were fixed at those of reference 1 and shown in table II with the exception of wall cooling ratio and specific impulse. The wall cooling ratio was varied from  $\eta = 0$  to 0.5, with primary emphasis being on the design value  $\eta = 0.25$ .

In the following sections the total thermal conductivity, given by equation (17), was used to evaluate liquid-fuel-mixture temperatures. The first section discusses the importance of turbulence and evaluates these temperatures for the case of uniform heat source distribution. The second section discusses the feasibility of fuel zoning, and the last section discusses the advantages of an insulating vapor layer between the liquid fuel and the solid support wall.

## Fuel-Mixture Temperatures With Uniform Heat Source Distribution

Temperature profiles in the liquid fuel mixture for uniform heat source distribution and assuming only molecular conduction are shown in figure 4. These profiles were calculated using equation (20) with  $\beta = 0$  and  $A = 0$ . Two important inconsistencies occur when only molecular conduction is considered:

(1) Since the boiling point of niobium carbide, the principal fuel-mixture component, is approximately  $13\,000^{\circ}\text{R}$  ( $7200^{\circ}\text{K}$ ) (see the appendix), figure 4 indicates that fuel boiling occurs in the liquid, resulting in an additional heat-transfer mode.

(2) The large radial temperature gradients shown in figure 4 coupled with a large radial acceleration field due to fuel-element rotation will cause free convection effects in the liquid near the propellant interface. This results in yet another additional heat-transfer mode. Both of these additional heat-transfer modes are ignored by an analysis based only on simple molecular conduction.

Temperature profiles for the same case but with turbulence included are shown in figure 5 and were calculated using equation (20) with  $\beta = 0$  and with the calculated value  $A = 11.0$ . A comparison of figures 4 and 5 indicates that liquid fuel temperatures near the support wall may be greatly overestimated when turbulence is ignored. The eddy conductivity is generally larger than the molecular conductivity (see fig. 2), so that both the temperature gradient and the maximum temperature in the liquid are significantly reduced. Thus, in the presence of eddy conduction, internal boiling will probably not occur. Also, the importance of free convection is greatly reduced. Therefore, when turbulence is accounted for, the two inconsistencies present in the laminar calculation are much less pronounced, or disappear altogether.

Support-wall temperatures for the uniform heat source distribution and various wall cooling ratios were calculated using equation (20) with  $\beta = 0$ , and they are illustrated in

figure 6. Values of wall temperature are plotted for the calculated turbulence coefficient  $A = 11.0$  and also for the  $A = 5.0$  and  $A = 20.0$ . Figure 6 indicates that, using the turbulence theory, wall temperatures are quite insensitive to the actual value of  $A$ . Thus, any uncertainties in fluid properties, or applicability of the turbulence theory, which may cause a deviation in the turbulence coefficient of as much as a factor of 2 from the calculated value  $A = 11.0$ , will not greatly affect the nature of the wall temperature curve.

The best current choice for support-wall material is graphite, which is a solid up to about  $7200^{\circ}\text{R}$  ( $4000^{\circ}\text{K}$ ). Thus, for a practical system, the wall temperature must be maintained below  $7200^{\circ}\text{R}$  ( $4000^{\circ}\text{K}$ ) with acceptable wall cooling ratios. Figure 6 indicates that at the reference value of  $\eta = 0.25$  the support wall must operate at  $9830^{\circ}\text{R}$  ( $5460^{\circ}\text{K}$ ), and that this temperature cannot be brought into the range of realistic material limits even by increasing the wall cooling fraction to  $\eta = 0.4$  at the loss of rocket specific impulse (see table I). It is thus clear that the feasibility of this radiating liquid-fuel rocket depends on a scheme for reducing the support-wall temperature at acceptable wall cooling rates.

## Fuel-Mixture Temperatures With Zoned Heat Sources And Time Dependence Of Zoned Fuel Concentrations

Within the restrictions imposed by system requirements, the wall temperature may be lowered considerably by zoning the fissioning fuel into a region in the liquid near the gas interface. Without considering for the moment the details of confining the fuel to a small region in the liquid, the steady-state temperatures with a step distribution of heat sources or fuel concentration within the liquid can be calculated from equations (19), (20), and (21). Figure 7 was constructed by using the calculated turbulence coefficient  $A = 11.0$  and a typical zone fraction  $\beta = 0.90$  (for fuel confined to one-tenth of the liquid thickness). A comparison of figures 6 and 7 indicates that, by fuel zoning with  $\beta = 0.90$  (and no fuel diffusion), support-wall temperatures are reduced about  $1200^{\circ}\text{R}$  ( $670^{\circ}\text{K}$ ) below those without zoning. Making the fuel region narrower, such that  $\beta > 0.90$ , would not measurably enhance these results.

Since fuel zoning is a potential means of reducing the wall temperature, the ability to actually confine nuclear fuel to a small fraction of the liquid thickness must be investigated. The fuel is initially solid and is zoned. Upon liquidification of the fuel mixture at rocket startup, steep radial fuel concentration gradients cause diffusion of fuel away from the zoning region and result in redistribution of fuel throughout the liquid mixture. The rate of this fuel redistribution is evaluated using the analysis of the TIME DEPENDENCE OF ZONED FUEL CONCENTRATIONS section.

The time dependence of fuel concentration with initial step distribution is calculated using equations (27) and (29). Normalized concentration profiles for the typical zoning fraction,  $\beta = 0.90$ , are shown for several dimensionless times after rocket startup in figure 8. Of particular interest is the time  $\theta_{1/2}$  when the fuel concentration at the wall reaches one-half the equilibrium value, that is, when  $C_o/\bar{C} = 0.5$ .

The quantity  $\theta_{1/2}$  is assumed to be a measure of the time after which the advantages of reduced wall temperature due to fuel zoning are lost. Figure 9 shows the time variation of fuel concentration at the solid wall for various  $\beta$  values. Values of fuel concentration were calculated using equation (29). The maximum duration of zoning effects is taken from figure 9 to be the largest possible value of  $\theta_{1/2}$ , equal to 0.14, which corresponds to the case where all the fuel heat sources are initially zoned into a very thin layer at the gas interface, or  $\beta \cong 1.0$ . With known mass diffusion coefficient this limit corresponds to  $t_{1/2} = (L^2\theta_{1/2}/D) = 0.14 (L^2/D)$ .

Assuming only molecular mass diffusion occurs and using the estimated value of  $D$  given in the appendix give the maximum duration of zoning effects as  $t_{1/2} = 25$  minutes. In reality, turbulent effects, which were shown previously to be an important mechanism of heat transfer, should be included in estimating the value of  $D$ . Thus when turbulence is accounted for, the maximum expected value of  $t_{1/2}$  becomes so small that any advantages of wall temperature reduction due to initial fuel zoning are expected to be lost within a fraction of realistic rocket operating life. On the basis of a simple mass diffusion model, it is thus concluded that initial fuel zoning cannot be expected to lower significantly the solid wall temperature over rocket operating life.

Several means of inhibiting the rapid redistribution of zoned fuel may be considered. If the NbC solvent, which has a lower density than the  $UC_2$  fuel, is replaced with a material having the same physical properties as NbC but a greater density than the  $UC_2$  fuel, it is conceivably possible that the rotating fuel element would act like a centrifuge. In effect, the lower density fuel would tend to collect in the region near the gas-liquid interface as desired.

An estimate of this effect was made using the centrifuge equation given in Bird, et al. (ref. 6). For the design radial acceleration of  $387 g_o$ , a fuel mixture depth of 0.0095 meter, and the extreme case of a solvent having twice the density of  $UC_2$ , the equilibrium fuel concentration in the centrifuge case was found to be only 6 percent greater at the gas interface than at the solid wall. Thus the centrifuge effect would not significantly inhibit the rates at which zoned fuel is redistributed by mass diffusion.

Another possible means of confining the fuel would be to float it on a denser substance which, although liquid, would not be wetted by the liquid fuel. Thus, surface tension effects would tend to confine the fuel to a layer resting on another liquid layer. However, even if such a more dense nonwetting substance could be found for this application,

turbulence, which would be induced in the liquid fuel and its support substance, would probably cause breakup and mixing of the fueled and unfueled layers, again redistributing the fuel and heat sources throughout the liquid.

Thus, for the possibilities just considered, it is clear that with initial fuel zoning the fuel redistributes itself throughout the liquid region of the fuel element shortly after rocket startup. Therefore, for the greater part of rocket operating life the fuel temperature distribution would be as shown in figure 5.

## Support-Wall Temperature With an Insulating Vapor Layer at the Liquid-Solid Interface

An alternative means of reducing support-wall temperature is by means of a vapor layer built up at the liquid-solid interface. The analytic details of generating such a vapor layer, whether by sublimation of a graphite support wall, or injection through a porous wall, are not treated here. However, a simple derivation in the analysis section leading to equation (31) indicates that the maximum thickness of a stable vapor layer that remains attached to the support wall is about 0.57 millimeter.

The temperature drop across a vapor layer was evaluated using the radiative heat-transfer analysis given in reference 4. The support-wall temperature was calculated for vapor layers of various optical thicknesses by using the values of liquid-mixture temperature  $T_0$  and heat flux  $q_0''$  at the wall taken from figure 5. The results are shown in figure 10. The actual value of optical thickness  $\chi$  corresponding to the vapor-layer thickness of 0.57 millimeter is difficult to estimate as pointed out in the analysis; however, a representative value was calculated assuming a carbon vapor layer at  $9000^\circ\text{R}$  ( $5000^\circ\text{K}$ ). The calculated value of  $\chi = 1.8$  is possibly an overestimate and should be experimentally verified. Support-wall temperatures for the assumed vapor layer are given by the curve for  $\chi = 1.8$  in figure 10. These estimates for a stable vapor layer at the support wall indicate a wall temperature of  $8500^\circ\text{R}$  ( $4720^\circ\text{K}$ ) for the design value  $\eta = 0.25$ . Also, a wall temperature of  $7200^\circ\text{R}$  ( $4000^\circ\text{K}$ ) may be achieved by increasing wall cooling to  $\eta = 0.32$ , which decreases specific impulse to 1250 seconds.

## Engine Performance Feasibility

The high support-wall cooling rates require the propellant to be preheated to some inlet temperature before entering the fuel element proper. Reference 1 gives the relation that results between rocket specific impulse and wall cooling ratio for the case where propellant inlet temperature is limited to a  $3500^\circ\text{R}$  ( $1940^\circ\text{K}$ ) maximum by rocket

structural material limits. This relation is given in table I.

The support-wall temperatures for the three principal cases considered are replotted from previous figures as functions of wall cooling ratio and the corresponding specific impulse in figure 11. The curve for fuel zoning is mainly of theoretical interest and cannot be physically realized due to rapid fuel redistribution rates.

Two points on these curves are especially important. For the case of unzoned fuel directly on the support wall, figure 11 indicates that, for the reference specific impulse of 1430 seconds, solid support-wall materials with structural limits above  $9830^{\circ}$  R ( $5460^{\circ}$  K) are required. The curve for the insulating vapor layer, while requiring further experimental verification, indicates that current wall materials, with a  $7200^{\circ}$  R ( $4000^{\circ}$  K) limit, may permit operation with a reduced specific impulse of 1250 seconds.

## CONCLUSIONS

This analysis of heat transfer in the liquid fuel mixture extends the work of reference 1 on a new radiating liquid-core nuclear rocket concept, which consists of a liquid carbide fuel mixture supported on the inside wall of a rotating tube. The axially flowing hydrogen propellant is heated by thermal radiation from the liquid surface. An expression for combined turbulent and molecular heat transfer in the liquid fuel was developed and then used to calculate temperatures at the solid support wall for a 1430-second specific impulse rocket with  $9500^{\circ}$  R ( $5280^{\circ}$  K) fuel surface temperature.

With turbulent mixing in the liquid fuel accounted for, support-wall temperature for the 1430-second rocket was  $9830^{\circ}$  R ( $5460^{\circ}$  K), well in excess of practical wall material limits.

With fuel zoned into one-tenth of the liquid thickness farthest from the support wall, it was found that wall temperatures are reduced about  $1200^{\circ}$  R ( $660^{\circ}$  K) by fuel zoning. However, a mass diffusion analysis indicates that fuel zoning could not be maintained over rocket lifetime. Thus, the advantages of reduced wall temperature due to fuel zoning cannot be physically realized.

The insulating effect of a stable vapor layer built up at the solid-liquid interface was also evaluated. The estimated value of radiation optical thickness for such a vapor layer is probably not very accurate; however, for the particular case studied it was found that wall temperatures were significantly reduced by a vapor layer at the wall. A specific impulse of 1430 seconds required a  $8500^{\circ}$  R ( $4720^{\circ}$  K) support-wall temperature; a specific impulse reduced to about 1250 seconds would require a more realistic  $7200^{\circ}$  R ( $4000^{\circ}$  K) wall temperature.

The final conclusions reached are as follows:

1. Turbulent mixing in the liquid fuel must be accounted for in the estimates of

support-wall temperature.

2. To realize a design specific impulse of about 1430 seconds, solid support-wall materials with melting points near  $9830^{\circ}$  R ( $5460^{\circ}$  K) must be developed.

3. The buildup of a vapor layer at the wall may permit use of current materials, such as graphite, for a support wall at  $7200^{\circ}$  R ( $4000^{\circ}$  K), but would probably reduce the attainable specific impulse to about 1250 seconds. The actual hydrodynamic and radiative heat-transfer characteristics of such an insulating vapor layer require further experimental verification.

Lewis Research Center,  
National Aeronautics and Space Administration,  
Cleveland, Ohio, October 12, 1967,  
122-28-02-18-22.

## APPENDIX

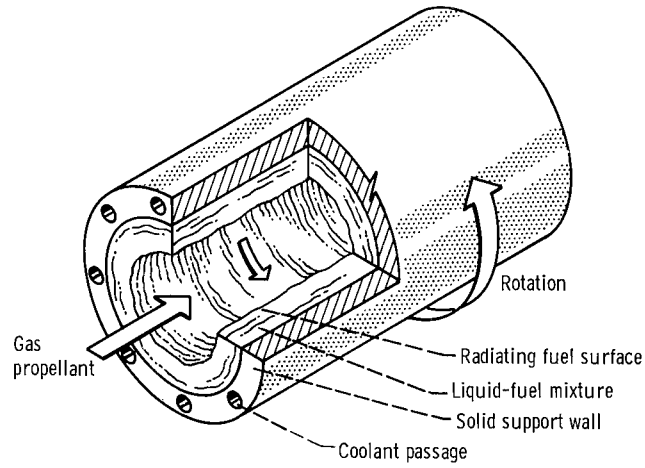
### LIQUID-FUEL-MIXTURE PROPERTIES

For determination of properties, the liquid fuel mixture is assumed to consist of liquid NbC at  $9000^{\circ}\text{R}$  ( $5000^{\circ}\text{K}$ ). Property data were taken from the following sources, and in most cases were estimated using semi-empirical relations from the indicated sources:

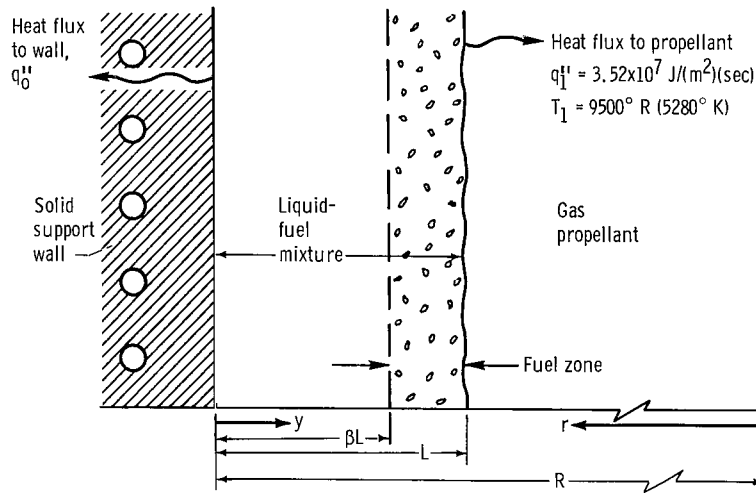
Melting point temperature, $^{\circ}\text{R}$ ( $^{\circ}\text{K}$ ) (ref. 7) . . . . .	6750 (3750)
Boiling point temperature (for 1 atm ( $1.01 \times 10^5 \text{ N/m}^2$ )), $^{\circ}\text{R}$ ( $^{\circ}\text{K}$ ) (ref. 7) . . . . .	8570 (4770)
Boiling point temperature (for 200 atm ( $2.02 \times 10^7 \text{ N/m}^2$ )), $^{\circ}\text{R}$ ( $^{\circ}\text{K}$ ) (ref. 8) . . . . .	13 000 (7200)
Density (estimated using ref. 7), $\rho_L$ , $\text{kg/m}^3$ . . . . .	7150
Specific heat (estimated using ref. 9), $C_{P_L}$ , $\text{J}/(\text{kg})(^{\circ}\text{K})$ . . . . .	585
Viscosity (estimated using ref. 10), $\mu_L$ , $(\text{N})(\text{sec})/\text{m}^2$ . . . . .	$4.75 \times 10^{-3}$
Molecular thermal conductivity (estimated using ref. 9), $k_L$ , $\text{J}/(\text{m})(\text{sec})(^{\circ}\text{K})$ . . . . .	43.3
Kinematic viscosity ( $\nu_L = (\mu_L/\rho_L)$ ), $\nu_L$ , $\text{m}^2/\text{sec}$ . . . . .	$6.77 \times 10^{-7}$
Prandtl number ( $\text{Pr}_L = (\mu_L c_{P_L}/k_L)$ ), $\text{Pr}_L$ . . . . .	0.0647
Surface tension (estimated using ref. 11), $\sigma$ , $\text{N/m}$ . . . . .	1.49
Molecular mass diffusion coefficient (estimated using ref. 12), $D$ , $\text{m}^2/\text{sec}$ . . . . .	$8.37 \times 10^{-9}$

## REFERENCES

1. Ragsdale, Robert G.; Kascak, Albert F.; and Donovan, Leo F.: Heat- and Mass-Transfer Characteristics of an Axial-Flow Liquid-Core Nuclear Rocket Employing Radiation Heat Transfer. NASA TN D-4127, 1967.
2. Wrobel, J. R.; and McManus, H. N., Jr.: An Analytic Study of Film Depth and Pressure Drop in Annular Two-Phase Flow. Developments in Mechanics. Vol. 1. Plenum Press, 1961, pp. 578-587.
3. Schlichting, Hermann (J. Kestin, trans.): Boundary Layer Theory. Fourth ed., McGraw-Hill Book Co., Inc., 1960.
4. Deissler, R. G.: Diffusion Approximation for Thermal Radiation In Gases With Jump Boundary Conditions. J. Heat Transfer, vol. 86, no. 2, May 1964, pp. 240-246.
5. Main, Roger P.; and Bauer, Ernest: Opacities of Carbon-Air Mixtures at Temperatures From 3000 - 10,000<sup>0</sup> K. J. Quant. Spectrosc. Radiat. Transfer, vol. 6, no. 1, Jan.-Feb. 1966, p. 1-30.
6. Bird, R. Byron; Stewart, Warren E.; and Lightfoot, Edwin N.: Transport Phenomena. John Wiley and Sons, Inc., 1960, p. 576.
7. Samsonov, G. V.: Handbook of High-Temperature Materials. Vol. II. Plenum Press, 1964.
8. Masser, Charles C.: Vapor-Pressure Data Extrapolated to 1000 Atmospheres ( $1.01 \times 10^8 \text{ N/m}^2$ ) 13 Refractory Materials with Low Thermal Absorption Cross Sections. NASA TN D-4147, 1967.
9. Neel, David S.; Pears, C. D.; and Oglesby, Sabert, Jr.: The Thermal Properties of Thirteen Solid Materials to 5000<sup>0</sup> F for their Destruction Temperatures. (WADD TR-60-924), Southern Research Inst., Feb. 1962, pp. 93, 118.
10. Grosse, A. V.: The Viscosity of Liquid Metals and An Empirical Relation Between Their Activation Energy of Viscosity and Their Melting Points. J. Inorg. Nucl. Chem., vol. 23, no. 3/4, 1961, pp. 333-339.
11. Grosse, A. V.: The Relationship Between the Surface Tensions and Energies of Liquid Metals and Their Critical Temperatures. J. Inorg. Nucl. Chem., vol. 24, no. 2, Feb. 1962, pp. 147-156.
12. Cahill, J. A.; and Grosse, A. V.: Viscosity and Self-Diffusion of Liquid Thallium from Its Melting Point to About 1300<sup>0</sup> K. J. Phys. Chem., vol. 69, no. 2, Feb. 1965, pp. 518-521.



(a) Conceptual representation of radiating fuel element.



(b) Nomenclature and general characteristics of analyzed fuel element.

Figure 1. - Liquid-core fuel element of nuclear rocket.

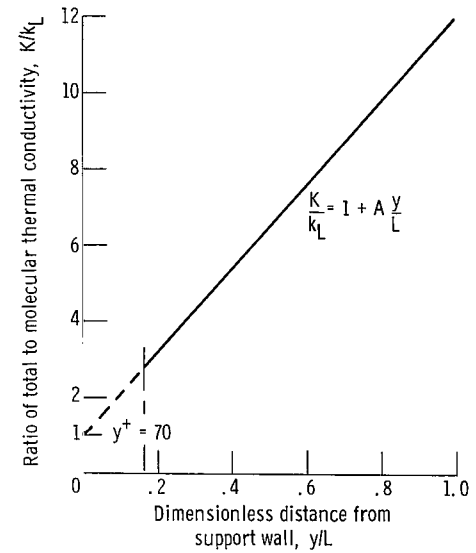


Figure 2. - Variation of molecular plus turbulent thermal conductivity with distance from support wall. Ratio of turbulent to molecular thermal conductivity,  $A = 11.0$ .

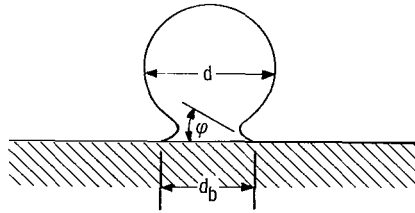


Figure 3. - Schematic of vapor bubble on support wall showing nomenclature.

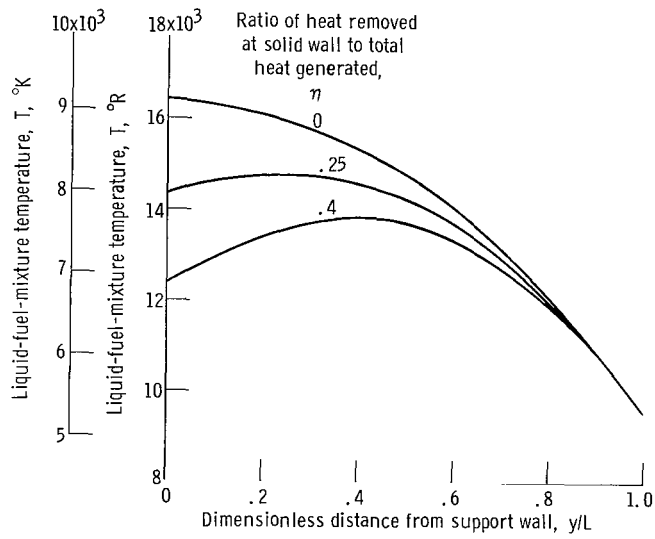


Figure 4. - Temperature profile in liquid fuel mixture for various wall cooling ratios with molecular conduction only and uniform heat source distribution. Ratio of turbulent to molecular thermal conductivity,  $A = 0$ ; fraction of liquid thickness which has no heat sources,  $\beta = 0$ .

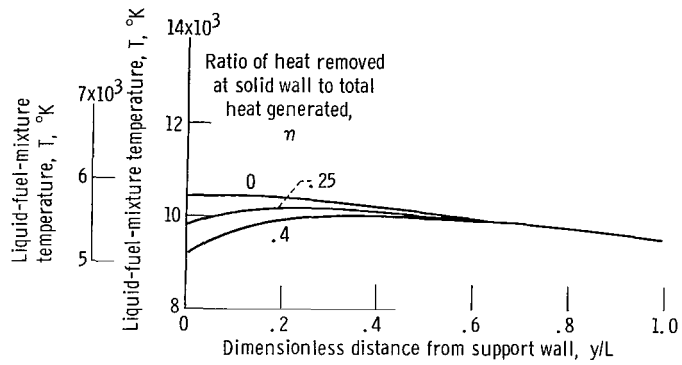


Figure 5. - Temperature profile in liquid fuel mixture for various wall cooling ratios with molecular plus turbulent heat transport and uniform heat source distribution. Ratio of turbulent to molecular thermal conductivity,  $A = 11.0$ ; fraction of liquid thickness which has no heat sources,  $\beta = 0$ .

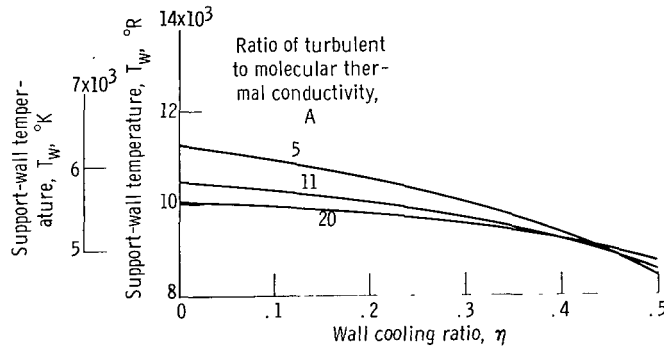


Figure 6. - Variation of support-wall temperature with wall cooling ratio for various turbulence coefficients and uniform heat source distribution. Fraction of liquid thickness which had no heat sources,  $\beta = 0$ .

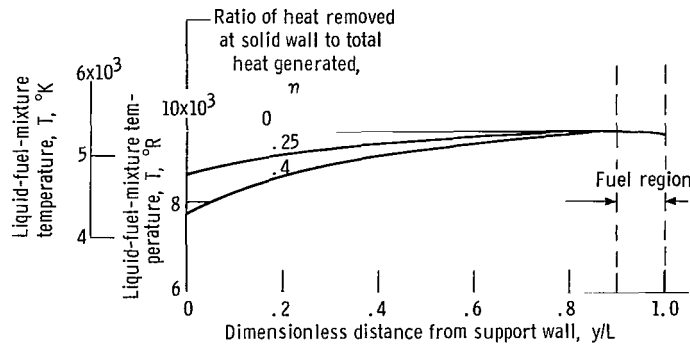


Figure 7. - Temperature profile in liquid fuel mixture for various wall cooling ratios with molecular plus turbulent heat transport and zoned heat sources. Ratio of turbulent to molecular thermal conductivity,  $A = 11.0$ ; fraction of liquid thickness which had no heat sources,  $\beta = 0.9$ .

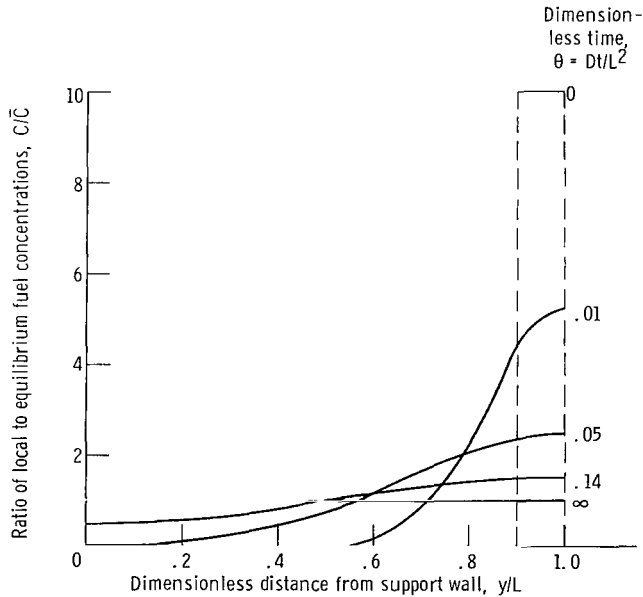


Figure 8. - Fuel concentration variation with dimensionless time with fuel zoned initially into one-tenth of liquid thickness. Fraction of liquid thickness which had no heat source,  $\beta = 0.9$ .

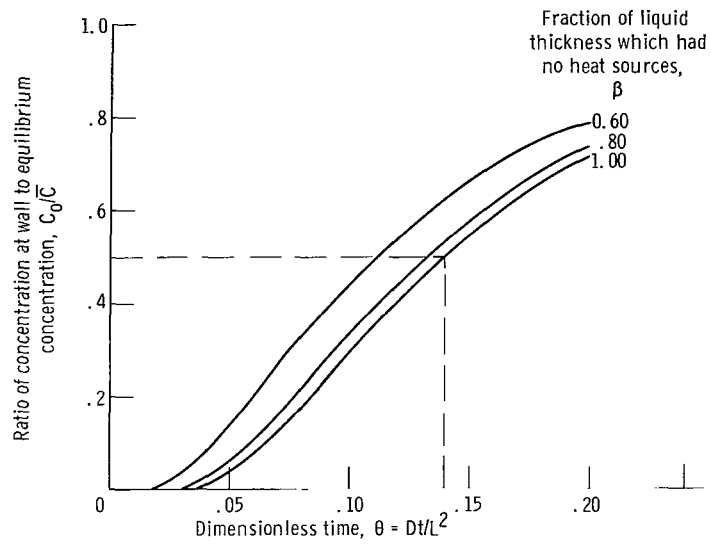


Figure 9. - Variation of fuel concentration at support wall with time for various zone fractions.

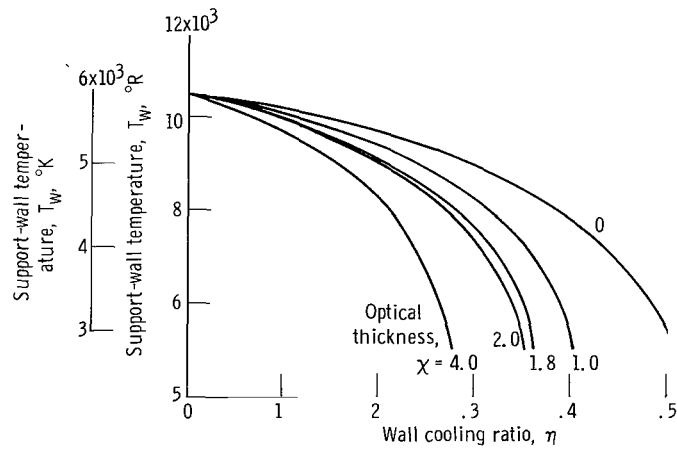


Figure 10. - Variation of support-wall temperature with wall cooling ratio for vapor layers of various optical thicknesses at wall. Ratio of turbulent to molecular thermal conductivity,  $A = 11.0$ ; fraction of liquid thickness which had no heat sources,  $\beta = 0$ .

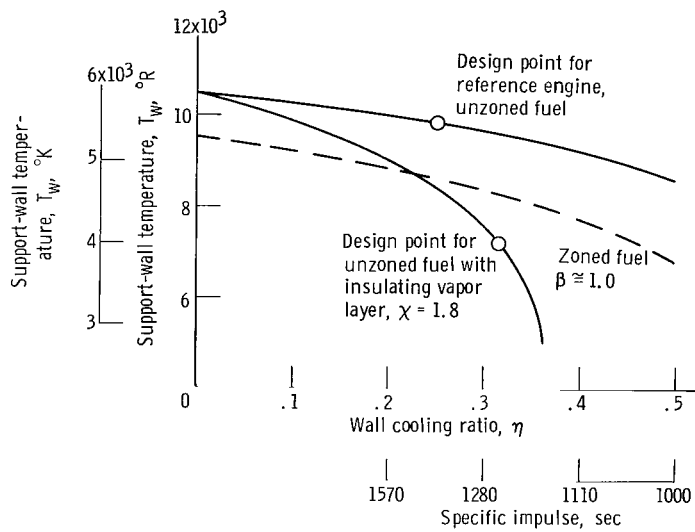


Figure 11. - Variation of support-wall temperature with wall cooling ratio and specific impulse for various cases analyzed and turbulent mixing included.

030 001 52 51 305 00909  
AIR FORCE WEAPONS LABORATORY/AFWL/  
KIRTLAND AIR FORCE BASE, NEW MEXICO 87117

ATTN: MISS MADEIRA E. CANOVA, CHIEF TECHNICAL  
LIBRARY/AFWL/

POSTMASTER: If Undeliverable (Section 158  
Postal Manual) Do Not Return

*"The aeronautical and space activities of the United States shall be conducted so as to contribute . . . to the expansion of human knowledge of phenomena in the atmosphere and space. The Administration shall provide for the widest practicable and appropriate dissemination of information concerning its activities and the results thereof."*

—NATIONAL AERONAUTICS AND SPACE ACT OF 1958

## NASA SCIENTIFIC AND TECHNICAL PUBLICATIONS

**TECHNICAL REPORTS:** Scientific and technical information considered important, complete, and a lasting contribution to existing knowledge.

**TECHNICAL NOTES:** Information less broad in scope but nevertheless of importance as a contribution to existing knowledge.

**TECHNICAL MEMORANDUMS:** Information receiving limited distribution because of preliminary data, security classification, or other reasons.

**CONTRACTOR REPORTS:** Scientific and technical information generated under a NASA contract or grant and considered an important contribution to existing knowledge.

**TECHNICAL TRANSLATIONS:** Information published in a foreign language considered to merit NASA distribution in English.

**SPECIAL PUBLICATIONS:** Information derived from or of value to NASA activities. Publications include conference proceedings, monographs, data compilations, handbooks, sourcebooks, and special bibliographies.

**TECHNOLOGY UTILIZATION PUBLICATIONS:** Information on technology used by NASA that may be of particular interest in commercial and other non-aerospace applications. Publications include Tech Briefs, Technology Utilization Reports and Notes, and Technology Surveys.

*Details on the availability of these publications may be obtained from:*

SCIENTIFIC AND TECHNICAL INFORMATION DIVISION  
NATIONAL AERONAUTICS AND SPACE ADMINISTRATION

Washington, D.C. 20546